International Journal of Greenhouse Gas Control 110 (2021) 103434

Contents lists available at ScienceDirect

International Journal of Greenhouse Gas Control

journal homepage: www.elsevier.com/locate/ijggc

# BECCS with combined heat and power: assessing the energy penalty☆

Kåre GUSTAFSSON [a,b,*], Ramiar SADEGH-VAZIRI [c], Stefan GRÖNKVIST [c], Fabian LEVIHN [b,d], Cecilia SUNDBERG [a,e]

[a] KTH – Royal Institute of Technology, Department of Sustainable Development, Environmental Science and Engineering (SEED), Stockholm, Sweden
[b] Stockholm Exergi, Stockholm, Sweden
[c] KTH – Royal Institute of Technology, Department of Chemical Engineering, Stockholm, Sweden
[d] KTH – Royal Institute of Technology, Department of Industrial Economics and Management, Stockholm, Sweden
[e] Swedish University of Agricultural Sciences (SLU), Department of Energy and Technology, Uppsala, Sweden

ARTICLE INFO

*Keywords*
Bio-energy with carbon capture and storage (BECCS)
$CO_2$ capture
Combined heat and power
Energy penalty
Chemical absorption
Potassium carbonate ($K_2CO_3$)
Modelling and simulation

ABSTRACT

Bio-energy with carbon capture and storage (BECCS) is widely recognised as an important carbon dioxide removal technology. Nevertheless, BECCS has mostly failed to move beyond small-scale demonstration units. One main factor is the energy penalty incurred on power plants. In previous studies, this penalty has been determined to be 37.2–48.6% for the amine capture technology. The aim of this study is to quantify the energy penalty for adding the hot potassium carbonate (HPC) capture technology to a biomass-fired combined heat and power (CHP) plant, connected to a district heating system. In this context, the energy driving the capture process is partially recovered as useful district heating. Therefore, a modified energy penalty is proposed, with the inclusion of recovered heat. This inclusion is especially meaningful if the heat has a substantial monetary value. The BECCS system is examined using thermodynamic analysis, coupled with modelling of the capture process in Aspen Plus™. Model validation is performed with data from a BECCS test facility. The results of this study show that the modified energy penalty is in the range of -3% to 7%. These findings could potentially increase the attractiveness of BECCS as a climate abatement option in a district heating CHP setting.

## 1. Introduction

Apart from afforestation and reforestation, the most recognised of the carbon dioxide removal technologies (CDRTs) is bio-energy with carbon capture and storage (BECCS) (IPCC, 2014). This technology captures and permanently stores the $CO_2$ released from the energy conversion of biomass, such as the $CO_2$ emitted from power stations (Kemper, 2015). Although BECCS is an important technology for climate change mitigation (Gregory et al., 2018), its deployment has thus far failed to move beyond small-scale demonstration units (Gough et al., 2018). A limited number of ethanol plants are an exception Global CCS Institute. Bioenergy and Carbon Capture and Storage. (accessed March, 15 2020). This failure can be attributed to technological and financial (Clarke et al., 2014), social (Honegger and Reiner, 2017), political (Fridahl, 2017) and ecological challenges (Hoegh-Guldberg and Hijioka, 2018). If BECCS is to be realised at scale, the thresholds of these challenges must be lowered.

The most significant challenge to the implementation of BECCS at bio-energy plants is the considerable investment cost and operational cost of carbon capture and storage (CCS) (Budinis et al., 2018). The need to withdraw low-grade steam and electricity to operate BECCS at a power plant is particularly detrimental, as it will incur an energy penalty and lower the overall efficiency of the power plant (Page et al., 2009). If the energy could be recovered and utilised, the cost of implementing BECCS could be lowered (Bui et al., 2017b).

Out of the plethora of potential carbon capture technologies, few are ready for implementation. In fact, the only technology that has been found to be ready for deployment at power stations is post-combustion absorption (Bui et al., 2018). Consequently, the only two full-scale CCS plants in operation at power stations both use this technique

DOIs of original article: https://doi.org/10.1016/j.ijggc.2020.103248, https://doi.org/10.1016/j.ijggc.2021.103433.

☆ The authors regrets that, due to circumstances out of their control, an old version of the presented article was published prematurely while the corresponding author was on a prolonged absence from work, due to having contracted severe long-COVID. The corresponding author would like to apologise for any inconvenience caused.

* Corresponding author:
*E-mail address:* kareg@kth.se (K. GUSTAFSSON).

https://doi.org/10.1016/j.ijggc.2021.103434

Available online 25 August 2021

(Mumford et al., 2015). Post-combustion technologies have the major advantage of being suitable for retrofitting to existing point sources of $CO_2$ (Mumford et al., 2015). The concept of retrofitting bio-energy plants has an appealing aspect: namely, that the energy conversion part of BECCS is already in place. Hence, the time for deployment could be shorter and the investment cost lower than for a new, complete BECCS deployment.

At present, research on BECCS within the energy sector is largely limited to power generation (Bhave et al., 2017; Cabral et al., 2019; Emenike et al., 2020), often in combination with the amine absorption technology (Budinis et al., 2018; Bui et al., 2017a; Pour et al., 2018; Sanchez and Callaway, 2016; Skorek-Osikowska et al., 2017), despite the tendency of amine absorbents to degrade in an oxidative environment (Borhani et al., 2015). As for how to perform energy integration between a carbon capture process and an energy conversion plant, studies on electrical power plants, such as those by Harkin et al. (2011); Kather (2016) and Bui et al. (2017a), have examined this topic.

If the ambition of deploying BECCS is broadened to combined heat and power plants (CHPs), absorbents other than amines could be an option. Levihn et al. (2019) suggest that the hot potassium carbonate (HPC) technology could be viable, since it would reduce the cost for capture and liquefaction by 17%. The main reason for this reduction is that the substantial energy requirement for flue gas compression, which is inherent to HPC technology, can be partly recovered as useful heat. Furthermore, a crucial advantage of HPC in the post-combustion application is the high resistance to oxidative degradation (Borhani et al., 2015). Previously, BECCS in CHPs has been studied in an industrial context, with a focus on part load and amine technology (Kuramochi et al., 2010). Unlike the case of power plants, energy integration between a CHP and a post-combustion carbon capture process has been little studied. This is surprising, since there is apparent potential for keeping the energy penalty at a low level by recovering useful heat. Ideally, this could lower the threshold for investments in BECCS and thereby increase its attractiveness as a climate mitigation option.

This study expands the BECCS research field into CHPs in the energy sector. The aim is to quantify the energy penalty of applying the HPC technology to a CHP plant in a district heating (DH) system.

## 2. The potassium carbonate process

The potassium carbonate process was developed in the 1940s–1960s at the U.S. Bureau of Mines (USBM) (Milidovich and Zbacknick, 2013). Co-workers Benson and Field produced the original publications on the process, such as an article by Benson et al. (1954). Hence, the process is also known as the Benfield process. The initial aim of the USBM was to facilitate cost-efficient removal of $CO_2$ and sulphuric compounds from synthesis gas, to allow for the production of liquid fuels from coal gasification (Milidovich and Zbacknick, 2013). Since then, the technology has been adopted for a number of different gas mixes (Speight, 2019). Worldwide, more than 700 units have been licenced based on the UOP Benfield™ technology, while at least another 150 units have been established with technologies from other companies (Smith et al., 2016).

The potassium carbonate process relies on a pressure difference (pressure swing) between the absorption and desorption of $CO_2$ (Smith et al., 2016). In the common application of synthesis gas purification, the feed gas is already highly pressurised. This allows the potassium carbonate process to operate at a temperature considerably above the atmospheric boiling point, which increases the reaction kinetics and lowers the energy demand (Smith et al., 2016). Due to the elevated temperature, the method has also become known as the hot potassium carbonate (HPC) process. Apart from the test facility described in this paper, which removes $CO_2$ from flue gases generated by biomass combustion, the HPC process has previously been demonstrated at pilot scale with flue gases from coal combustion (Mumford et al., 2012; Smith et al., 2014).

A simplified flow diagram of the Benfield process is shown in Fig. 1. The feed gas enters the bottom of the absorber where it meets the absorbent, in a counter-current flow. $CO_2$ is absorbed into the potassium carbonate solution, as shown in reaction (1) (Smith et al., 2016). Subsequent chemical reactions (2–5) trap the $CO_2$ in the solution. The resulting summary reaction (6) is exothermal.

$$CO_2(g) \rightleftarrows CO_2\ (aq) \tag{1}$$

$$CO_2(aq) + OH^-(aq) \rightleftarrows HCO_3^-(aq) \tag{2}$$

$$CO_2(aq) + H_2O(l) \rightleftarrows H_2CO_3\ (aq) \tag{3}$$

$$H_2CO_3(aq) + H_2O(l) \rightleftarrows HCO_3^-(aq) + H_3O^+(aq) \tag{4}$$

$$HCO_3^-(aq) + H_2O(l) \rightleftarrows CO_3^{2-}(aq) + H_3O^+(aq) \tag{5}$$

$$CO_2(g) + CO_3^{2-}(aq) + H_2O(l) \rightleftarrows 2HCO_3^-(aq) \tag{6}$$

The rich (loaded) absorbent leaves the absorber at the bottom and is depressurised before it enters the top part of the stripper. In the stripper, reaction (6) is reversed in part due to the lower pressure, which causes the $CO_2$ to transfer to the gas phase. The $CO_2$ leaving the top of the stripper contains water vapour, which is partly recovered in the condenser and brought back to the stripper.

Since the reversal of the absorption is endothermic, it is necessary to add thermal energy to the stripper. Heat is usually supplied through low-grade steam that condensates in the reboiler (Puxty and Maeder, 2016). The required amount of heat is called the heat duty ($q_{reb}$) of the process, and is the sum of three terms (Oexmann and Kather, 2010):

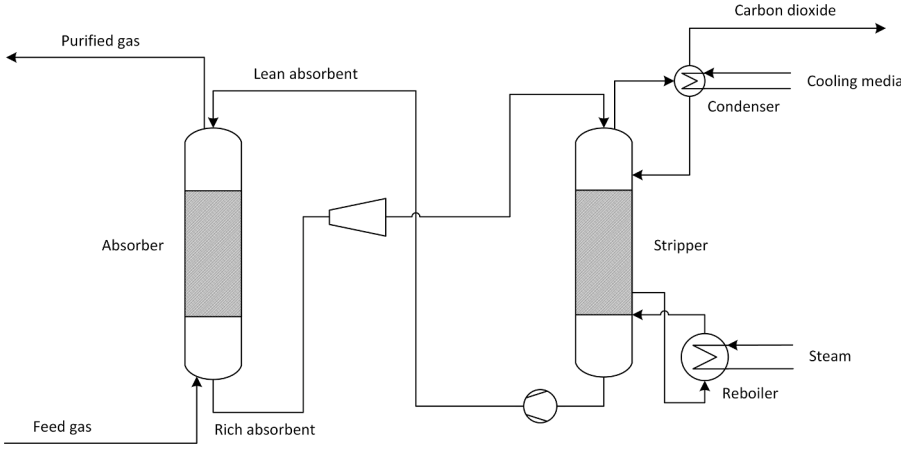


**Fig. 1.** A simplified illustration of the original Benfield process, adapted from Kohl and Nielsen (1997).

$$q_{reb} = q_{sens} + q_{vap,H_2O} + q_{abs,CO_2} \quad (7)$$

The first term ($q_{sens}$) is the sensible heat for bringing the absorbent to the operating temperature of the stripper. For the HPC process, this term can be relatively low, as the process is often designed with similar temperatures in the absorber and the stripper (Smith et al., 2016). The second term ($q_{vap,H_2O}$) is the heat required to vaporise the water that is mixed with the $CO_2$ leaving the column. This vaporisation of water is by far the most energy intense of the three terms (Kohl and Nielsen, 1997). The last term ($q_{abs,CO_2}$) is the overall heat needed to break the chemical bonds created in the absorber and to enable the $CO_2$ to transfer to the gas phase – that is, to reverse the summary reaction (6). This third term is relatively small in the case of potassium carbonate, in comparison with other absorbents (Mumford et al., 2015).

## 3. Method

This paper is aimed at quantifying the energy penalty of adding carbon capture to a biomass-fired CHP plant connected to a district heating system. The applied methodology consisted of a thermodynamic analysis of the defined systems, coupled with modelling of the carbon capture processes in Aspen Plus. The results of the modelling were validated with experimental data from a HPC carbon capture test plant and from the literature. The method encompassed the following steps:

1) Defining the BECCS systems;
2) Defining the modified energy penalty and other performance indicators;
3) Collecting data on the CHP plant and the district heating system;
4) Modelling and simulating the full-scale carbon capture processes in Aspen Plus;
5) Validating the full-scale Aspen Plus capture models against test plant data and literature; and
6) Modelling the energy integration between the CHP and the CCS systems, including calculation of the energy penalty, other performance parameters and the monetary cost-of-energy for the $CO_2$ capture.

The main analysis was performed on a defined base case with parameters from an existing CHP. Two different varieties of the carbon capture process were included in the base case: one basic concept and one more advanced concept. The reference case was the CHP plant without added carbon capture.

### 3.1. The BECCS systems

The two studied systems were limited to the CHP plant and the carbon capture equipment, differing only in the configuration of the capture process. The main components were the biomass-fired boiler, the flue gas cleaning equipment with flue gas condensation (FGC), the steam turbine, the carbon capture equipment including compression of the flue gas, and the $CO_2$ liquefaction plant (Fig. 2).

In Fig. 2, the parameters marked with (k) were kept constant, while the parameters marked with (Δ) were varied between the BECCS systems. Parameters marked with (δ) were varied within the analysis of each BECCS system. Unlike the fuel input, the district heating and electric power output varied. The variations in those outputs were mainly influenced by the variation of the steam and electric power need of the capture processes. For example, a high steam requirement resulted in a lower electric output, since less steam passed through the turbine. Similarly, a high need for electric power in the capture process yielded less electric output from the system. For the district heating output, the opposite was true. An increased need for steam and electric power gave a higher output of district heating, since more heat was recovered inside the capture process. The amount of captured $CO_2$ was constant due to unvarying fuel input and a fixed $CO_2$ capture rate (Eq. 15).

### 3.2. The energy penalty of carbon capture

Capturing $CO_2$ from the flue gas of an energy conversion plant requires energy input (Bui et al., 2017b). This results in a lowering of the net energy efficiency ($\eta_{PPCC}$) of the plant. For regular electric power generation plants with CCS, the net energy efficiency can be expressed as a percentage of the fuel lower heating value ($LHV_f$) (Cabral and Mac Dowell, 2017):

$$\eta_{PPCC} = 100 \times \frac{P_{PP} - P_{CC}}{m_f \times LHV_f} \quad (8)$$

where $P_{PP}$ is the net electric output from the power plant without carbon capture, $P_{CC}$ is the electric output lost due to the capture process and $m_f$ is the mass flow of the fuel. Note that the power used by the carbon capture process consists of two parts (Page et al., 2009). The first part is the electric power requirement of the capture process, which could be substantial for the HPC process, due to the reliance on elevated pressures for absorption. The second part is incurred by the steam that is withdrawn from the power plant turbine and utilised in the capture process, leading to a reduction of the electric power production.

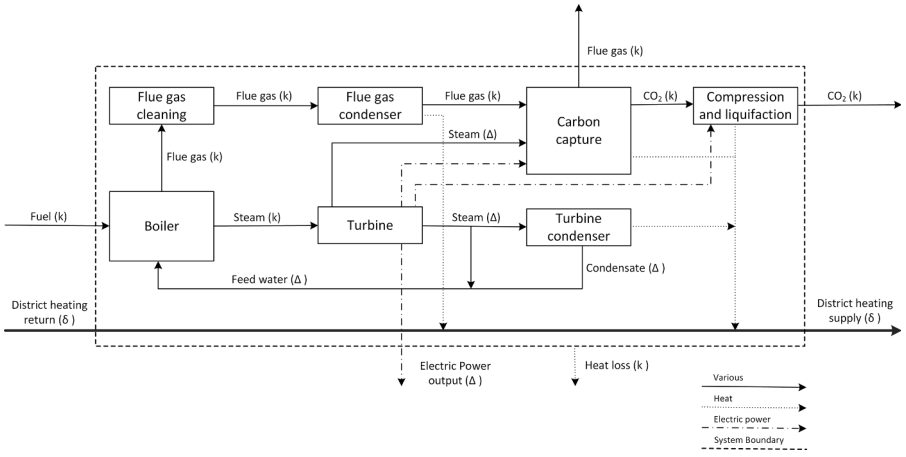


**Fig. 2.** The dashed box shows the limitation of the studied BECCS systems. The label (k) identifies streams with constant material and energy flows in the analysis, while (Δ) identifies streams that were varied between the basic and advanced capture processes. District heating parameters, labelled with (δ), were varied within the analysis of each capture process.

One useful expression for quantifying and comparing the energy requirement of adding carbon capture at a power plant is the energy penalty (Page et al., 2009), which is a relative expression:

$$Energy\ penalty\ = 100 \times \frac{P_{PP} - P_{PPCC}}{P_{PP}} \quad (9)$$

where $P_{PPCC}$ is the electric power output from the power plant after carbon capture has been attached.

While Eq. (9) is useful for studying plants producing only electric power, a modified definition of the energy penalty was required for this study. To define such modified energy penalty, there is a need to have an expression for the CHP total efficiency with CCS. Since a CHP plant produces both heat and electric power, it is natural to include the heat into Eq. (8). This yields an expression for the efficiency of a CHP plant with carbon capture, $\eta_{CHPCC}$:

$$\eta_{CHPCC} = \frac{P_{CHP} + Q_{CHPCC} - P_{CC} + Q_{rec}}{m_f \times LHV_f} \quad (10)$$

where $P_{CHP}$ is the net electric power output from the CHP plant without carbon capture, $Q_{CHPCC}$ is the net district heating ouput from the CHP after CCS has been added, and $Q_{rec}$ is the useful, recoverable heat from the capture process. The term $Q_{CHPCC}$ is the sum of the heat generated in the steam turbine condenser and the heat recovered from the flue gases in the FGC. Due to the recovery of the latent heat in the water vapour in the FGC, $\eta_{CHPCC}$ can have a value above 100%. This since the $LHV_f$ is defined as the heat of combustion of the fuel with the fuel moisture content and the water from the combustion reaction in vaporised form in the flue gases. As an alternative, Eq. 10 can be expressed with the higher heating value ($HHV_f$), which is defined as the heat of combustion with the water vapour in condensed form. In that case, $\eta_{CHPCC}$ will have a value below 100%, (Eq. 11).

$$\eta_{CHPCC} = \frac{P_{CHP} + Q_{CHPCC} - P_{CC} + Q_{rec}}{m_f \times HHV_f} \quad (11)$$

Incorporating the heat into Eqs. (10) and (11) is only meaningful if the heat has a monetary value and is of suitable quality – that is, has the required district heating supply temperature. Therefore, low-grade heat that would require heat pumps to meet the supply temperature was ignored when calculating recoverable heat. Furthermore, it was assumed that the lost electric power production can be supplied by other production units within the wider electrical power system, and that the increased amount of heat produced can be utilised within the district heating system. In addition, only cases where the CHP operates at full load have been examined, i.e. part load operation has not been taken into consideration. From Eqs. (9) and (10), it follows that the energy penalty of a CHP plant with CCS can be expressed as:

$$CHP\ energy\ penalty\ = 100 \times \frac{P_{CHP} + Q_{CHP} - P_{CHPCC} - Q_{CHPCC} - Q_{rec}}{P_{CHP} + Q_{CHP}} \quad (12)$$

Where $Q_{CHP}$ is the district heating output from the CHP plant without carbon capture and $P_{CHPCC}$ is the net electrical power output from the CHP plant after carbon capture has been added. In addition, to provide a broad set of performance indicators, the following metrics were included: the net electrical efficiency for a CHP with CCS ($\eta_{el,net\ CHPCC}$) (Eq. 13); and the preservation of electric power output from the CHP after adding CCS (Eq. 14).

$$\eta_{el,net\ CHPCC} = \frac{P_{CHPCC}}{m_f \times LHV_f} \quad (13)$$

$$CHP\ power\ preservation\ = \frac{P_{CHPCC}}{P_{CHP}} \quad (14)$$

### 3.3. The CHP plant and the district heating system

The analysis of the energy penalty was made on an existing CHP. Such an approach was considered to make the results of the study less theoretical, and follows the line of thought of Page et al. (2009). A CHP plant situated in Stockholm was chosen. The plant, known as CHP 8, generates heat for the city's district heating network, as well as electric power. It should be noted that for CHP 8 there are few restrictions regarding the prioritisation between production of heat and production of electric power, except for process characteristics such as the alpha value and the turbine minimum load. There is, for example, no need to supply a specific amount of electricity at all times. Therefore, the operational mode can be gradually switched from combined heat and power production to heat only, at the cost of power production at a rate of 1:1 (Levihn, 2017). Moreover, a CHP plant typically operates as a base load unit if situated in a district heating system, which normally allows the produced heat to be fully utilised. The fuel used in CHP 8 is wood chips, which are produced from secondary biomass derived from forestry residues. The plant was deemed especially suitable since CHP 8 is being considered for full-scale BECCS implementation (Gustafsson,

**Table 1**
Data on CHP 8.

| Parameter | | | Note |
|---|---|---|---|
| Fuel type[1] | Wood chips | | |
| Fuel input, $LHV_f$ [1] | 362.1 | MW | |
| Fuel input, $HHV_f$ [1] | 451.5 | MW | |
| Fuel heating value, $LHV_f$ [1] | 8.1 | MJ/kg | As received, including moisture |
| Fuel heating value, $HHV_f$ [1] | 10.1 | MW | |
| Steam temperature[1] | 558 | °C | |
| Steam pressure[1] | 13.6 | MPa | |
| Flue gas flow, 3.4% $O_2$, dry gas (dg) [1] | 441 000 | $Nm^3/h$ | Reference: 0°C, 101.32 kPa |
| Flue gas temperature[1] | 33.6 | °C | In stack, after flue gas condensation (FGC) and humidification. Calculated value. |
| Turbine electric power output, gross[1] | 124.8 | MW | From generator |
| Turbine condenser heat output[1] | 207.9 | MW | |
| Flue gas condenser heat output | 105 | MW | Calculated |
| District heating return temperature[1] | 38.2 | °C | |
| District heating temperature, into turbine condenser[1] | 59 | °C | |
| District heating temperature, out of turbine condenser[1] | 81 | °C | |
| Flue gas composition, wet gas (wg)[1]: | | | In stack |
| Carbon dioxide | 16.0 | vol% | |
| Oxygen | 3.2 | vol% | |
| Water | 5.3 | vol% | |
| Nitrogen and inert gases | 75.5 | vol% | |

Reference:
[1] Stockholm Exergi (2016)

2018). As a further advantage, there is a test facility for carbon capture installed at the plant. This test facility was utilised for validation of the full-scale Aspen Plus models in this study.

The data on CHP 8 (Table 1) were mostly taken from the performance tests (Stockholm Exergi, 2016). The data are appropriate to use, since a performance test is a special period of operation during which all noteworthy performance parameters are documented with a higher degree of precision. Moreover, it is conducted by a third party, thus ensuring an impartial evaluation of the plant performance.

In this study, a generalised district heating system was chosen for the analysis, instead of a specific system. The motivation for this choice was to generate results that are more widely applicable. Therefore, Swedish average temperature levels were chosen for the base case (Table 2). To broaden the perspective even further, an analysis was performed of the impact of different district heating temperature levels (Table 2) on the energy penalty.

Concerning the district heating flow rates, it was supposed that the CHP plant was part of a site with additional production units (Fig. 3). More specifically, it was assumed that heat pumps or similar low-grade heat production units were available. The function of such units is partly to ensure a sufficient flow of district heating water at the right temperature level to the turbine condenser, and partly to add flexibility into the system. In addition, it was assumed that a heat-only boiler (HOB) was available to increase the district heating temperature from turbine condenser output level to supply level. The functionality provided by these units is certainly needed to optimise the performance of a CHP plant, irrespective of the addition of CCS. For example, if there is no HOB, the district heating temperature from the turbine condenser would have to be increased to meet the supply temperature. In effect, this would reduce the possible electric power production from the turbine. Overall, the system in Fig. 3 is representative of the production optimisation of advanced urban multi-energy carrier systems (Levihn, 2017).

The adjoining production units were not part of the studied system when calculating the energy penalty. Instead, they were used for examining adverse effects that could render the results of the study invalid. Therefore, during the calculations, checks were performed to ensure that the low-grade heat source and the HOB were not utilised beyond the need for the reference case without CCS. To clarify further, it was a boundary condition of the base case that recovering heat from the CCS system should not require adding excessive amounts of heat at unreasonable temperature levels. Fig. 3 shows the district heating supply temperature, 86 °C, that had to be met regardless of adding CCS to the system. Unlike the base case, the further analysis of the impact of district heating temperatures on the energy penalty allowed the HOB to be utilised beyond its usage in the reference case. This in order to understand the effects of district heating temperatures on HOB utilisation.

Regarding the operational priority within the system, the performance of the BECCS plant was calculated first. Thereafter, the low-grade heat source and the HOB were adjusted to meet the required flows and temperature levels.

Table 2 summarises the various district heating temperatures. Apart from the base case, the impact on the energy penalty of a low- and a high-temperature district heating network was analysed. The low-temperature case was taken as the Danish average and the high-temperature case was taken from Basel, in Switzerland. The Basel network represents a system that is moving towards lower temperatures – in this case, from the second to the third generation district heating system, as defined by Lund et al. (2018). The chosen temperatures for Basel are the expected values for 2025, after the development of the system (iwb, 2020).

**Table 2**
District heating temperature levels.

| Parameter | | | Note |
|---|---|---|---|
| Base case | | | |
| District heating return[1] | 47 | °C | Swedish average |
| District heating supply[1] | 86 | °C | Swedish average |
| Low case | | | |
| District heating return[1] | 43 | °C | Danish average |
| District heating supply[1] | 78 | °C | Danish average |
| High case | | | |
| District heating return[2] | 55 | °C | Basel 2025 |
| District heating supply[2] | 100 | °C | Basel 2025 |

References:
[1] (Gadd and Werner, 2014),
[2] (iwb, 2020)

### 3.4. Modelling and simulation of the carbon capture process

Aspen Plus was used to simulate a full-scale HPC carbon capture plant. The choice of Aspen Plus was partly motivated by its dominance in simulations of steady-state carbon capture systems in published scientific papers (Tumilar et al., 2016).

For this study, an equilibrium model adjusted with the Murphree Efficiency (ME) was used for the absorber. The rationale for using this simpler type of model was that the purpose of the simulations was not to design the internals of the absorber and the stripper, which would require a rate-based model (Isa et al., 2018), but rather to generate data for the overall mass and energy balance of the capture plant. For this purpose, an equilibrium model has been found to serve well (Fosbøl et al., 2017). Moreover, Wu et al. (2018) and Ooi (2008) have shown that an equilibrium model can generate valid results when compared with a rate-based model, if adjusted with the ME. The ME was acquired from the test plant trials, as explained in Section 3.5.

In Aspen Plus, two different full-scale potassium carbonate system were modelled, one basic (Fig. 4a) and one more advanced (Fig. 4b). The aim of modelling two systems was to understand how efficiency enhancements of the capture system would affect the energy penalty and other performance indicators. The ambition was to quantify a performance difference between the process configurations, not necessarily to find the optimal configurations. The simulations were performed using the Aspen Plus in-built electrolyte non-random two-liquid (ENRTL) model, which is widely accepted among researchers (Isa et al., 2018).

The major difference between the basic and advanced systems was that the latter was equipped with lean vapour compression (Kohl and Nielsen, 1997). This is a common measure for reducing the heat duty by partly generating steam within the capture process itself, thus lowering the steam requirement for the reboiler. Steam generation is achieved by flashing the lean absorbent and compressing the vapour phase before injecting it back into the stripper.

For the basic capture system, the function of the absorber and stripper was similar to the simple system (Fig. 1). However, the condensate water from the flash tank was returned directly to the lean absorbent, instead of being returned to the stripper. Another modification was intercooling of the absorber, which was added to increase the loading capacity of the absorbent and to avoid excessive water vaporisation from the absorber top.

Since absorption is done at elevated pressure, it was necessary to include compression of the flue gas in the simulations. The pressure increase was simulated as two stages, which reduces the energy need due to the intercooling between the compressors. Moreover, this opened up the possibility of driving the compressors with energy carriers other than electricity, since the individual compressors were then of a suitable size to fit in-system available energy carriers. The first compressor was driven by a high-pressure steam turbine, with steam supplied from the CHP. The outlet, low-pressure (0.4 MPa) saturated steam, was used as part of the energy supply to the reboiler. The second compressor was driven by the flue gas expander, which recovers energy from the purified flue gas. Having a flue gas expander added another benefit. It allowed for the flue gas temperature to be lowered further than what is normally possible with a stand-alone CHP with FGC. In other words, there was a

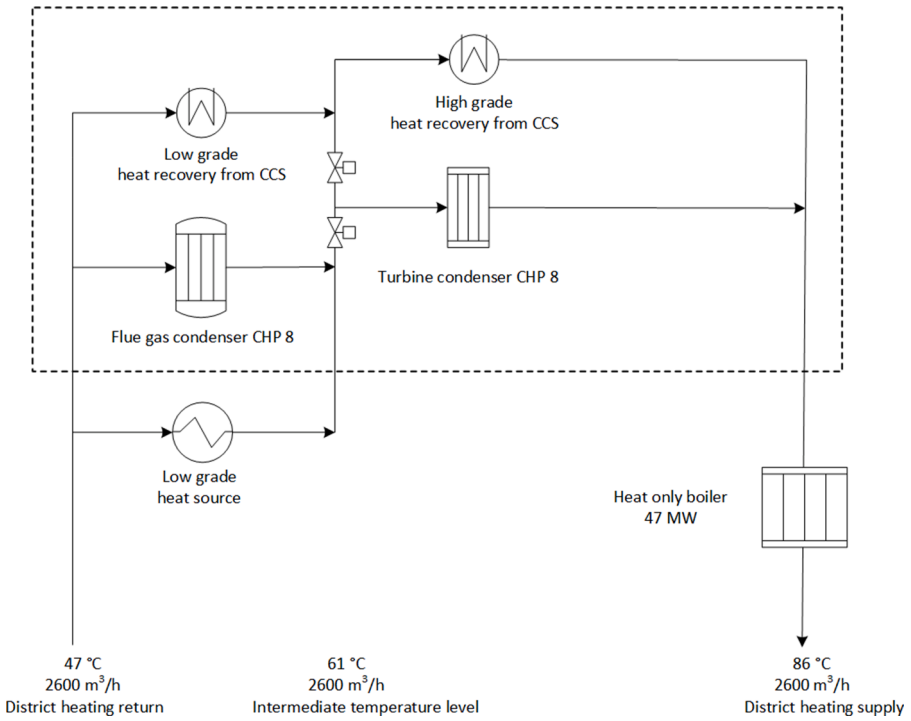


**Fig. 3.** The generalised district heating system, with the studied system in the dashed box. The numbers that are presented applies to the base case with the basic capture process.

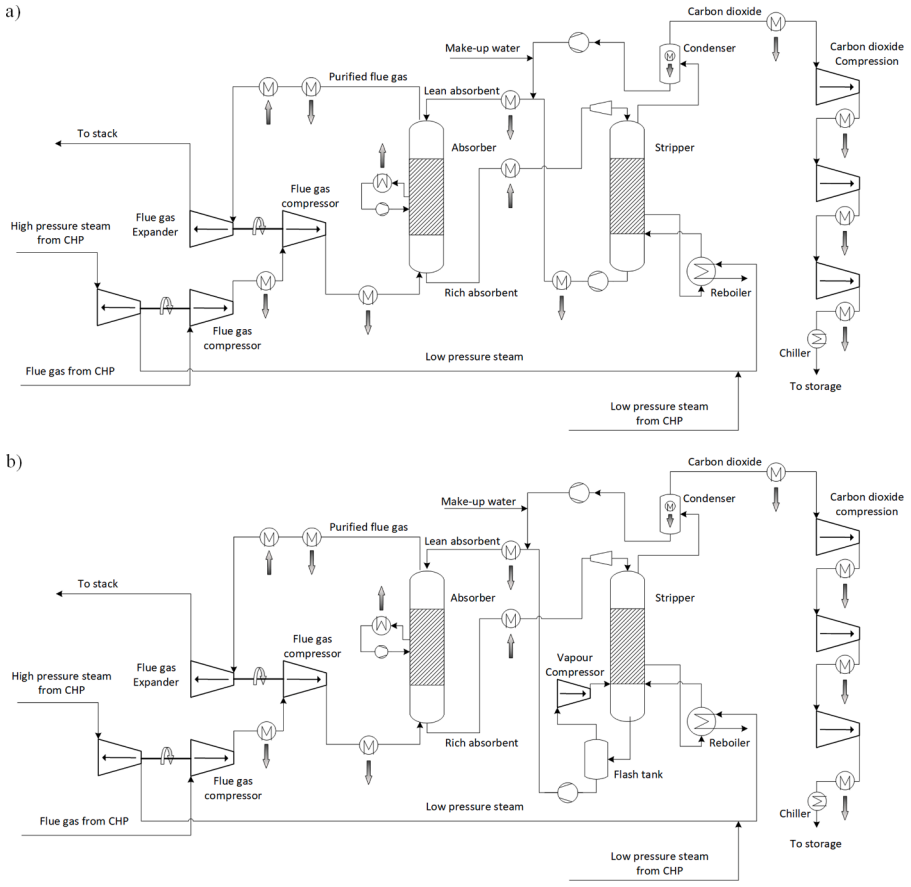


**Fig. 4.** The simulated a) basic and b) advanced carbon capture processes. The process streams from which heat can potentially be recovered at district heating temperature levels are marked with arrows pointing out of the heat exchanger symbol. Where heat input is required, the arrows point into the heat exchanger symbol.

net addition of useful energy output from the flue gas, compared to the reference case. This opened up for the possibility of achieving a net increase in energy output from the studied system.

The compression and liquefaction of the captured $CO_2$ was designed similarly to a process modelled by Cabral and Mac Dowell (2017), with a three-step compression with intercooling. The $CO_2$ was pressurised to 1.6 MPa and cooled down below −26°C, for storage and further transport. The pressure and temperature data are consistent with the preliminary requirements for Northern Lights, the geological storage site outside Norway, which is currently being developed (Equinor, 2020).

The simulations in Aspen Plus were performed with the requirement of achieving 90% $CO_2$ removal. The target was set based on the findings of Harkin et al. (2011), which show that the heat duty increases drastically beyond a 90% capture rate. The expression for the capture rate is shown in Eq. (15), which has been adapted from the work of Mumford et al. (2012).

$$Capture\ rate = 100 \times \frac{CO_2\ flow\ out\ from\ stripper}{CO_2\ flow\ in\ feed\ gas} \quad (15)$$

To give some initial stability to the Aspen Plus model and to avoid too wide of an approach, the absorbent strength was fixed to 30 wt% $K_2CO_3$. Kohl and Nielsen (1997) conclude that this is the recommended solution strength, if unwanted precipitation of salts is to be avoided. The strength of the potassium carbonate solution will influence the amount of $CO_2$ that can be captured at a given solvent flow rate, as shown by Tosh (1959). This is an important aspect, since lowering the liquid-to-gas ratio (L/G) in the absorber generally lowers the required reboiler heat duty. This can be derived from Eq. (7), where $q_{sens}$ will increase with a higher flowrate of absorbent.

To achieve a low L/G while simultaneously reaching a certain capture rate, a satisfactory loading of the absorbent with $CO_2$ must be accomplished. The loading is expressed as the mol% of captured $CO_2$ in relation to the absorbent (Wu et al., 2018)

$$Loading = \frac{mole\ of\ CO_2\ absorbed}{mole\ of\ K_2CO_3\ in\ absorbent} = \frac{[HCO_3^-]}{[K^+]} \quad (16)$$

Apart from the data on solution strength, there is little conclusive data in the literature for designing post-combustion absorption with potassium carbonate. Studies by Bohloul et al. (2014) and Bohloul et al. (2017) are two exceptions. These studies indicate that, from an absorption capacity perspective, the optimal pressure in the absorber is around 0.6–0.8 MPa. Higher pressures provide little added effect in terms of capacity. Another limitation in this study was to keep the lean solvent loading above 18%. Harkin et al. (2011) found that below this value the reboiler heat duty increases rapidly.

With these starting points, balancing of the capture process was done in the Aspen Plus model by varying design parameters, using the in-built sensitivity tool. The varied parameters were primarily the lean solvent inlet temperature, lean solvent loading, L/G, absorber pressure and number of stages in the absorber. The strategy for designing the absorber was to keep the L/G low, in order to decrease the reboiler heat duty and thus the steam consumption. This strategy was justified since the goal was to reach a fixed capture rate, with the column size being one of the variables. Others have employed a different approach, for example Harkin et al. (2011) and Artanto et al. (2012), where the absorber was fixed and the optimum heat duty was sought by allowing the capture rate, among other parameters, to vary.

It should be noted that the absorber pressure and temperature for post-combustion absorption will have to be substantially lower than those for traditional acid gas removal. In the latter application, the feed gas is inherently pressurised to 3–6 MPa (Borhani et al., 2015). Such a high pressure provides a sufficient driving force to dissolve $CO_2$ even at high temperatures close to the boiling point of the absorbent, at 100–140°C. For post-combustion, the pressure must be lower to avoid spending an unreasonable amount of energy on compressing the flue gases. From this, it follows that the absorber temperature must be reduced in order to provide an adequate net driving force to dissolve $CO_2$.

### 3.5. Validation of the Aspen Plus models with data from the test plant and the literature

In this study, test plant trials were performed to obtain a valid ME for adjustment of the full-scale Aspen Plus equilibrium models, a procedure recommended by (Ooi, 2008). The test plant used in this case was commissioned in December 2019 by the utility company Stockholm Exergi. It is located at Värtaverket, in central Stockholm, and captures around 4 kg of $CO_2$ per hour from a flue gas slipstream originating from CHP 8. Its configuration is similar to the simple process in Fig. 1.

The validation of the full-scale Aspen Plus models consisted of the following steps:

1) Performing test plant trials with operating parameters reflecting the full-scale models in order to acquire performance data;
2) Developing an equilibrium model of the test plant in Aspen Plus;
3) Inserting data from the test plant trials into the Aspen Plus test plant model;
4) Fine tuning the Aspen Plus test plant model with a ME to align model capture rate with test plant capture rate;

**Table 3**
Test plant operating parameters and corresponding parameters for the full-scale Aspen Plus models, compared with a non-exhaustive list of relevant literature data.

| Parameter | Test plant | Basic Aspen model | Advanced Aspen model | Literature | |
|---|---|---|---|---|---|
| Flue gas temperature | 39 | 42.5 | 42.5 | | °C |
| Flue gas composition: | | | | | |
| Carbon dioxide[1] | 7–18 | 16.0 | 16.0 | | vol% (wg) |
| Oxygen | 2–9 | 3.2 | 3.2 | | vol% (wg) |
| Water | 3–6 | 5.3 | 5.3 | | vol% (wg) |
| Nitrogen and inert gases | 74–77 | 75.5 | 75.5 | | vol% (wg) |
| Absorbent concentration of $K_2CO_3$ | 25–30 | 30 | 30 | 30[2] | wt% |
| Lean absorbent loading (Eq. 16) | 27–68 | 20 | 20 | 18-27[3] | mol % |
| Rich absorbent loading (Eq. 16) | 29–71 | 76 | 76 | | mol % |
| Absorber top temperature | 72 | 65 | 65 | 50–75[4] | °C |
| Absorber top pressure | 0.7 | 0.7 | 0.7 | 0.6-0.8[5], 0.8[4], 1.05[6] | MPa |
| Absorber, number of stages | 2 | 59 | 59 | | |
| Absorber liquid-to-gas ratio L/G | 5 | 4 | 4 | | |
| Stripper top temperature | 101 | 94 | 93 | | °C |
| Stripper top pressure | 0.12 | 0.13 | 0.13 | 0.12[2], 0.25[3] | MPa |

[1] The concentration of $CO_2$ in the flue gas was set to different levels, in order to simulate operating conditions in different parts of a full-scale absorber column.
[2] (Kohl and Nielsen, 1997),
[3] (Harkin et al., 2011),
[4] (Smith et al., 2012),
[5] (Bohloul et al., 2017),
[6] (Bryngelsson and Westermark, 2009),

5) Adjusting the Aspen Plus full-scale models with the ME acquired in point 4; and
6) Performing additional validation of the full-scale Aspen Plus models against the data from Bartoo (1984).

In the test plant trials, operating conditions such as L/G, temperatures and pressures was set close to those of the columns in the full-scale Aspen models. Table 3 shows the data used for the basic and advanced full-scale capture models, compared with the actual conditions of the test plant and with relevant, non-exhaustive, data found in literature.

One of the restrictions of the test plant was the height of the packing in the absorber, at 1.16 m. This limited the capture rate to around 10%, while the aim for the full-scale simulation was to have 90% capture rate. From this, it follows that a full-scale column could not be simulated by the test plant with just one point of operation. As a remedy, the test plant trials were expanded to include operation with several different $CO_2$ inlet concentrations and with different levels of lean absorbent loading. In effect, this approach made it possible to mimic the operating conditions of several sections throughout a full-scale absorber. The different levels of inlet $CO_2$ concentration was achieved by diluting the flue gas with air. This explains the wide range of oxygen, nitrogen and water vapour levels given for the test plant trials in Table 3.

Similarly to the full-scale models, Aspen Plus equilibrium models were built to simulate the test plant trials. One Aspen model was built for each trial, since parameters, such as lean loading and $CO_2$ inlet concentration, were varied between the trials.

The MEs for the different trials were then calculated with the Aspen Plus test plant models. The procedure was to insert the data obtained from the test plant, i.e. absorbent solution strength, temperatures, pressures, L/G, flue gas composition and lean absorbent loading. Thereafter, the ME was adjusted in the Aspen Plus model until the rich absorbent loading in the model matched that of the specific test plant trial. This procedure aligned the capture rate between the aspen test plant model and the specific test plant trial.

In Table 4 both the lean and rich absorbent loadings are shown for seven selected test plant trials with different lean absorbent loading. The loadings are compared with the calculated loadings from the test plant Aspen Plus models. As can be seen, they match reasonably well. Therefore, it was concluded that the Aspen Plus models were able to accurately simulate the test plant performance. The presented trials were selected because they matched the lean and rich loading of the absorbent at certain stages throughout the full-scale column in the Aspen Plus basic model. In addition, the $CO_2$ inlet concentration for the specific test plant trial approximately matched that of the corresponding stage in the full-scale absorber. An important consideration in this context is that a specific ME is only valid close to the pressure and temperature for which it has been calculated, as these parameters affect the mass transfer rate. Therefore, pressure and temperatures were set at similar levels for the test plant and full-scale Aspen Plus models, as can be seen in Table 3.

The values for the MEs obtained from the Aspen Plus calculations are shown in Table 4. The variation was higher than expected, between 0.023–0.076. More importantly, the variation does not display any discernible trend. Typically, a continuous variation of the ME along the height of the column should be expected, as shown by Al-Ramdhan (2001). After scrutiny of the solvent sampling and analysis procedure, it was concluded that the variations were likely to be a result of inaccuracies in the titration method, rather than from real variations in the process. With this in mind, an ME of 0.04 was chosen to be used for both the basic and the advanced full-scale Aspen Plus simulations. This value is lower than all the measured MEs, except one. Consequently, it was considered a conservative approach.

As an additional measure, the chosen ME was compared with the literature. Wu et al. (2018) found the ME to be as low as 0.01; however, the conditions for those tests were less beneficial, compared to those of the test plant trials in this study, having atmospheric pressure and ambient temperatures in the absorber. Working with more advantageous parameters, Ooi (2008) found that the ME was between 0.05 and 0.25. Those findings were based on existing industrial acid gas removal absorbers, operating at 7 MPa and 110°C. In yet another study, Al-Ramdhan (2001) found the ME to be between 0.04 and 0.08, using operational data from others, at 2.6 MPa and around 108°C. The results of Al-Ramdhan (2001), Ooi (2008) and Wu et al. (2018) indicate that the determined ME in this study is in line with what has been found in other experimental settings, as well as in industrial applications.

Despite the plausible robustness of the above validation, an analysis was performed to see how a change of the ME influences the heat duty of the simulated processes. The resultant heat duties were then compared with the work of Bartoo (1984). This comparison was done in an effort to determine whether the heat duties complied with industrial processes, such as natural gas sweetening. To explain further, it was assumed that the heat duties for the basic and advanced carbon capture processes were comparable with those of industrial processes. This is not necessarily true, as the conditions in the strippers differ. Nevertheless, it was reasoned that only the first term, $q_{sens}$, in Eq. (7) was expected to differ. As this term is small compared with $q_{vap,H2O}$ in the same equation, the assumption was deemed to be justified, as long as the respective heat duties were well within the range of the data from Bartoo (1984).

In Fig. 5, a comparison is made between expected heat duties, as indicated by Bartoo (1984), and calculated heat duties for the Aspen Plus full-scale models, for a range of MEs. Fig. 5 shows that the heat duties are well within the ranges of Bartoo (1984), for both the basic capture process and the more advanced process. Moreover, the heat duty is only mildly affected by the ME. This implies that from an energy requirement point of view the value of the ME is not critical within this range. Therefore, setting the ME to 0.04 in this study was confirmed as being reasonable. In contrast to the heat duty, the capture rate is strongly influenced by the ME at lower values. This was to be expected, since additional absorber stages would be needed to compensate for the lower ME, in order for the same capture rate to be achieved. Such an adaption of the number of absorber stages would cause the heat duty to become constant over the range of the ME in Fig. 5.

**Table 4**
Data on lean and rich absorbent loading for the test plant trials and resulting Murphree efficiencies.

| Trial point | Lean loading, test plant (mol%) | Lean loading, test plant Aspen model (mol%) | Rich loading, test plant (mol%) | Rich loading, test plant Aspen model (mol%) | Matching stage in full-scale Aspen basic model[1] | Murphree efficiency |
|---|---|---|---|---|---|---|
| 1 | 26.9 | 26.6 | 28.9 | 28.5 | 19 | 0.050 |
| 2 | 32.8 | 32.9 | 35.7 | 35.7 | 28 | 0.059 |
| 3 | 37.4 | 37.5 | 40.0 | 40.0 | 33 | 0.051 |
| 4 | 40.1 | 39.6 | 42.9 | 42.4 | 35 | 0.076 |
| 5 | 45.0 | 45.0 | 46.0 | 46.1 | 39 | 0.023 |
| 6 | 57.2 | 56.3 | 60.1 | 59.2 | 47 | 0.040 |
| 7 | 67.8 | 67.0 | 70.5 | 69.7 | 54 | 0.041 |
| Average | | | | | | 0.049 |

[1] Matching primarily refers to lean and rich loading, but also to the $CO_2$ concentration in the flue gas. The total number of stages in the absorber is 59.

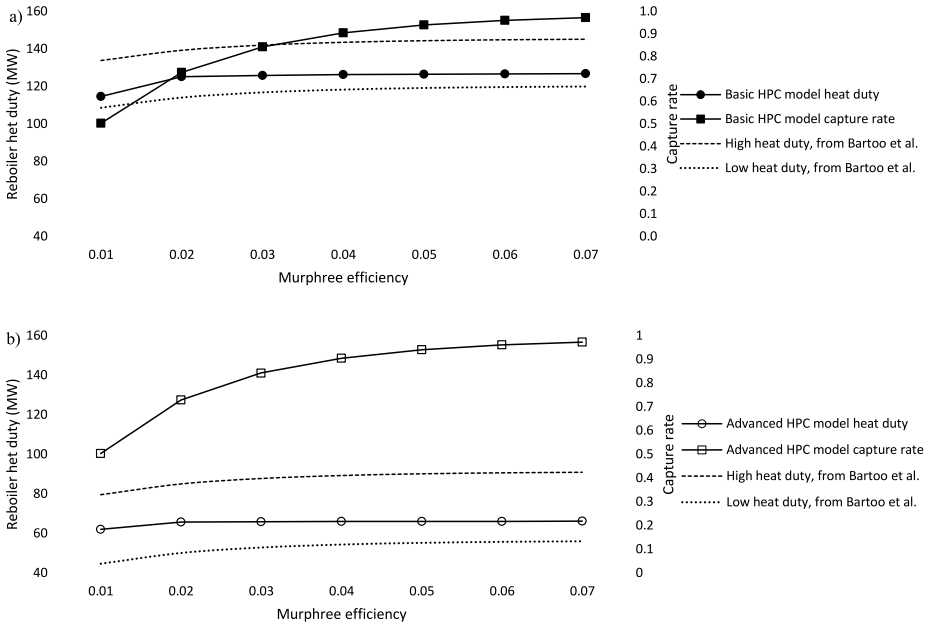


**Fig. 5.** The reboiler heat duty and $CO_2$ capture rate as a function of the absorber ME for the Aspen Plus simulations of (a) the basic HPC process and (b) the advanced HPC process. The dotted lines show the expected upper and lower limits of the heat duty for industrial carbon capture processes. These limits have been adjusted with the change in $q_{abs,CO_2}$ due to the change in capture rate.

### *3.6. Energy integration of the capture process with the CHP and the monetary cost-of-energy for capturing $CO_2$*

Fig. 2 shows the integration between the CHP and the CCS process, whereas Fig. 3 gives an overview of how the CHP and the CCS fit within the wider production of district heating. As can be seen in Fig. 2, the required amounts of steam, heat and electricity for the capture process were generated by the CHP. In addition, steam, heat and electricity generated by the CCS process itself were utilised within the capture process to enhance the efficiency. The low-pressure (LP) steam for the reboiler was mainly supplied by withdrawing high-pressure (HP) steam before the CHP turbine. To reach the correct temperature and pressure, the HP steam was passed through a steam turbine driving the first flue gas compressor. Neveux et al. (2017) have found this solution to be efficient for reducing the need for electric power. Any remaining steam demand in the basic capture process was de-superheated, incurring electric generation efficiency losses. De-superheating was necessary because the turbine lacks the capability to extract enough steam to supply the basic capture process at the correct pressure. Conversely, for the advanced capture process, the turbine bleed-off capacity was found to be sufficient for supplying additional LP steam.

The heat integration calculation was performed in Microsoft Excel®. The minimum approach temperature was set to 5°C for liquid-liquid heat exchangers and condensers, 10°C for gas-liquid heat exchangers and 15°C for gas-gas heat exchangers. These values are in the range suggested by Turton et al. (2018). Radiation and convection heat losses amounting to 0.5% of the input energy were used for both the CHP and the CCS system. This assumption was based on the performance test made on CHP 8 (Stockholm Exergi, 2016). No efficiency loss in the electrical system was considered.

The energy integration model allowed the CHP energy penalty (Eq. 12) to be calculated, along with the other performance parameters defined in Section 3.2. Based on these parameters, a calculation was made of the monetary cost-of-energy for the $CO_2$ capture. The monetary cost-of-energy was defined as the monetary net loss or gain in revenues from the sum of heat and electric production, when integrating CCS with the CHP. In these calculations, the base monetary value of both electricity and heat was set to 40 € per MWh. While the value of heat was kept constant, the value of electricity was increased stepwise to a maximum of 160 € per MWh. These numbers are in alignment with those used by Bui (2020). Naturally, depending on the contextual setup of different electric power and district heating systems, the monetary base value levels for heat and electricity can be different from those assumed here. It should be noted that the value of generated electric power differs from wholesale power market prices, which include additional fees for taxes and distribution. Likewise, the value of generated heat is relative to the substituted heat production, rather than the wholesale price.

## 4. Result

### *4.1. Energy penalty and other performance indicators*

The performed thermodynamic analysis showed that the CHP energy penalty (Eq. 12) was in the range of -3% to 7% (Table 5 and 6). Here, a negative number shall be interpreted as an increase in the total useful energy output from the studied system. The possibility of a slight increase in the energy output is mainly a result of the configuration of the capture process (Fig. 4), which allows for additional recovery of energy from the flue gas. Normally, the amount of energy that can be recovered is limited by the temperature of the district heating return flow and the combustion air humidifier, which both are utilised for cooling the flue gas in the FGC. With the suggested configuration in Fig. 4, it is possible to lower the outlet flue gas temperature even further, by producing electric power from the pressurised flue gas with an expander. Moreover, the water content in the outgoing flue gases is lower than in the incoming due to the heat exchanger set-up, allowing additional amounts of heat to be recovered.

For comparison, the common electricity-based energy penalty (Eq. 9) was calculated for the CHP, and was found to be in the range of 51–71% (Table 5). The reason for the difference in energy penalty between Eqs. (9) and (12) is that utilised electric power and steam can be recovered as useful heat into the district heating system.

Apart from the energy penalty, additional performance indicators were quantified (Table 4). The advanced capture process was found to be the better performing process on all accounts. It was particularly interesting that the electrical efficiency differed substantially between

**Table 5**
Data on CHP 8 without and with CCS.

| Parameter | CHP 8 alone (reference) | With basic CCS | With advanced CCS | |
|---|---|---|---|---|
| District heating temperature (return/supply) | 47/86 | 47/86 | 47/86 | °C |
| Fuel input, $LHV_f$ | 362.1 | 362.1 | 362.1 | MW |
| Fuel input, $HHV_f$ | 451.5 | 451.5 | 451.5 | MW |
| Turbine electric power output, gross[1] | 125 | 62 | 83 | MW |
| Turbine electric power output, net[1] | 110 | 36 | 50 | MW |
| Turbine condenser heat output[2] | 208 | 120 | 149 | MW |
| Flue gas condenser heat output | 88 | 88 | 88 | MW |
| CCS heat recovery | – | 163 | 123 | MW |
| Total heat output | 296 | 371 | 360 | MW |
| Energy efficiency, $LHV_f$ (Eq. 10) | 112.1 | 112.5 | 113.3 | % |
| Energy efficiency, $HHV_f$ ( Eq. 11) | 89.9 | 90.2 | 90.9 | % |
| Electrical efficiency, net ( Eq. 13) | 30.3 | 9.9 | 13.7 | % |
| Energy penalty, CHP (Eq. 12) | – | -0.4[3] | -1.1[3] | % |
| Energy penalty, power plant (Eq. 9), for comparison | – | 67.4 | 54.8 | % |
| Power preservation, CHP ( Eq. 14) | – | 32.6 | 45.2 | % |
| Reliance on HOBs to meet district heating supply temperature | 47 | 47 | None | MW |

[1] The turbine electric power output was adjusted with the impact of the district heating inlet temperature and flow rate to the turbine condenser.
[2] The approximation was made that the turbine condenser heat output is independent of the district heating return temperature, within the studied temperature interval.
[3] A negative number means that the total useful energy output from the studied system is increased, rather than decreased.

the two capture processes, and was almost 50% higher for the advanced process. Nevertheless, the electrical efficiency was still halved compared with the reference system. Another noteworthy point was that adding CCS did not increase the dependency on HOBs for meeting the required supply district heating temperature, compared with the reference. On the contrary, for the advanced process, the need for HOBs disappeared.

### 4.2. The influence of district heating temperatures

An analysis was performed on how the district heating return and supply temperatures affected the energy penalty of adding carbon capture to the CHP plant. In Table 6, it can be seen that all parameters are positively impacted by a low-temperature network, when compared with the base case in Table 5. The opposite is also true: a high-temperature system affects all parameters negatively. In addition, it was found that the need for HOBs, to increase the district heating supply temperature, disappears in the low-temperature case. In contrast, for the high-temperature case, there is a dramatic increase of the need for HOBs.

### 4.3. The monetary cost-of-energy for carbon capture

In Fig. 6 it is shown how the monetary cost-of-energy for capturing carbon dioxide relates to the difference in monetary value of electric

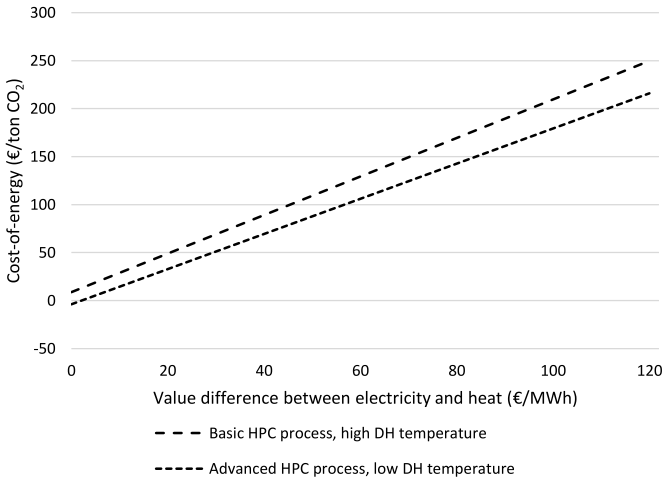


**Fig. 6.** The monetary cost-of-energy for the basic capture process with high district heating temperature (55°C return and 100°C supply) and the advanced capture process with low district heating temperature (43°C return and 78°C supply), in relation to the monetary value difference between electric power and heat. For both electricity and heat, the monetary base value was set to 40 € per MWh. The value of heat was kept constant at 40 € per MWh, while the value of electricity was increased stepwise to a maximum of 160 € per MWh.

**Table 6**
Analysis of the impact of district heating temperatures.

| Parameter | Basic CCS with low-temperature system | Basic CCS with high-temperature system | Advanced CCS with low-temperature system | Advanced CCS with high-temperature system | |
|---|---|---|---|---|---|
| District heating temperature (return/supply) | 43/78 | 55/100 | 43/78 | 55/100 | °C |
| Fuel input, $LHV_f$ | 362.1 | 362.1 | 362.1 | 362.1 | MW |
| Turbine electric power output, gross[1] | 65 | 58 | 88 | 79 | MW |
| Turbine electric power output, net[1] | 39 | 32 | 55 | 46 | MW |
| Turbine condenser heat output[2] | 123 | 118 | 152 | 141 | MW |
| Flue gas condenser heat output | 97 | 64 | 97 | 64 | MW |
| CCS heat recovery | 155 | 162 | 114 | 135 | MW |
| Total heat output | 375 | 344 | 363 | 340 | MW |
| Energy efficiency, $LHV_f$ (Eq. 10) | 114.5 | 104.1 | 115.6 | 106.7 | % |
| Energy efficiency, $HHV_f$ (Eq. 11) | 91.8 | 83.5 | 92.7 | 85.5 | % |
| Electrical efficiency, net (Eq. 13) | 10.8 | 8.9 | 15.3 | 12.6 | % |
| Energy penalty, CHP (Eq. 12) | -2.1[3] | 7.1 | -3.1[3] | 4.8 | % |
| Power preservation, CHP (Eq. 14) | 35.8 | 29.5 | 50.6 | 41.7 | % |
| Reliance on HOBs to meet district heating supply temperature | None | 194 | None | 220 | MW |

[1] The turbine electric power output was adjusted with the impact of the district heating inlet temperature and flow rate to the turbine condenser.
[2] The approximation was made that the turbine condenser heat output is independent of the district heating return temperature, within the studied temperature interval.
[3] A negative number means that the total useful energy output from the studied system is increased, rather than decreased.

power and heat, for the most favourable and the most unfavourable of the analysed cases. Here, the cost-of-energy is defined as the monetary net loss or gain in revenues from the sum of the produced heat and electricity, when integrating CCS with the CHP. As expected, a low difference in value between electricity and heat is highly beneficial for the cost-of-energy of carbon capture. For equal monetary values of electricity and heat, at 40 €/MWh, the monetary cost-of energy for the carbon capture is around -4 €/ton of $CO_2$ for the advanced capture process within a low temperature DH network. For the basic process within a high temperature DH network the monetary cost-of energy is around 9 €/ton of $CO_2$. This difference grows as the value gap between electricity and heat increases.

## 5. Discussion

BECCS is widely recognised as one of the key methods to facilitate carbon dioxide removal, which is a necessity if global temperature is to be kept within relatively safe levels (IPCC, 2018). However, many deterring factors hinder development. Of these, the costs for investment and operation are especially impeding, as there are no apparent economic returns (Gustafsson, 2018). Therefore, it is of interest to lower the costs for operating BECCS facilities and thereby lower the threshold for investments. This study investigated whether the energy penalty of integrating CCS with a biomass-fired CHP plant in a district heating setting could be lower than what has been found in other applications, thus contributing to such cost reductions. The energy penalty, which normally only includes the reduction of electricity output, was modified to include the useful heat (Eq. 12). This was motivated by the fact that a CHP plant has two valuable products: heat and electric power. The study was performed using thermodynamic analysis coupled with process modelling of the HPC carbon capture technology in Aspen Plus.

The results showed that the CHP energy penalty was in the range of -3% to 7% (Table 5 and 6). This is generally lower than the findings of other studies examining the amine carbon capture in combination with electric power stations, utilizing pulverized coal (PC) as a fuel. In those studies, which largely focused on non-standard advanced steam cycles, the theoretical energy penalty was found to be 15–28% (Page et al., 2009). The explanation for the lower energy penalty in this study is that a large proportion of the steam and electricity utilised in the capture process could be recovered into the district heating system as useful heat. In addition, the capture process configuration (Fig. 4) allowed for recovering further energy from the flue gas, compared to a stand-alone CHP. This explains why some of the cases in this study have a negative energy penalty, i.e. a gain in energy output from the CHP-CCS system. For the sake of transparency, the conventional energy penalty based on electric power (Eq. 9) was also calculated. By that definition, the energy penalty was found to be in the range of 55–67% (Table 5). As a comparison, Page et al. (2009) calculated the energy penalty to be 37.2–48.6% for real-world, sub-critical PC power plants with the amine capture technology. The high energy penalty when considering only electric power (Eq. 9) in this study probably explains why the HPC process has been little studied for post-combustion capture at power plants.

From a monetary cost-of-energy perspective, it is reasonable to believe that BECCS could be deployed at a lower cost in a CHP and district heating setting than in corresponding power plants settings. From this follows that the need for monetary incentives to reach a sufficient return on investment could be lower. Naturally, the validity of these statements is highly dependent on the difference in the monetary value of heat and electricity in the specific system. Essentially, a low value difference between electricity and heat will also yield a low, or even negative, monetary cost-of-energy for the capture process (Fig. 6). This finding is in general agreement with the findings of Bui (2020). In the specific context of this study, it was found that the cost-of energy was -4 to 9 €/ton of $CO_2$, if the value of both electricity and heat was set to 40 €/MWh. The advanced capture process in combination with a low district heating temperature network was the more advantageous, due to its lower energy penalty and higher electrical efficiency. In conclusion, optimization of the capture process is likely to be worthwhile if monetary cost-of-energy reductions are sought.

The CCS processes that were modelled in the full-scale Aspen Plus models could have been more advanced. This can be deduced from Fig. 5, where it can be seen that the reboiler heat duty might be further decreased to the lower levels found by Bartoo (1984). In a real-world plant, further improvements such as multistage lean compression (Mildovich and Zbacknick, 2013), split flow arrangements of the absorber and the stripper, and multiple strippers could be evaluated (Moullec and Neveux, 2016), to name a few examples. Drawing on the results of this study, such measures would probably not affect the overall energy penalty dramatically, but rather increase the electrical efficiency of the system.

A notable result of this study was that the implementation of the HPC capture process at a CHP does not increase the dependency on auxiliary HOBs at average Swedish district heating temperature levels. This effect stems from the possibility of recovering heat at elevated temperatures from the HPC process. Still, these results should be interpreted with caution, as it was also shown that the requirement for HOBs is strongly dependent on the district heating temperature levels. Consequently, the demand for HOBs will vary in a real district heating network in which the temperatures are fluctuating. The same is true for the energy penalty, which will also change with temperature levels. A dynamic study on how district heating temperature levels influence the energy penalty would therefore be valuable. Whether a reduced need for HOBs could motivate moving towards low-temperature district networks will have to be evaluated in relation to the individual district heating system. However, it can be concluded that low-temperature networks are well worth exploring when considering the implementation of CCS, as there are other benefits, such as improvement of the electrical efficiency of the BECCS system.

Iterative calculations, in which the results from the heat integration were allowed to influence the design of the capture system, were not performed in this study. The findings of Harkin et al. (2011) suggest that such an optimisation could decrease the overall energy need. For example, an increase of the stripper pressure could lead to a higher preservation of electric power production from the CHP, since the carbon dioxide compression work would be reduced. Another option that was not investigated is to integrate mechanical heat pumps into the BECCS system. Such a strategy would recover more heat at the further expense of electric power.

## 6. Conclusion

In this study, the energy penalty for establishing carbon capture at CHP plants in district heating systems was found to be -3% to 7%, if the useful heat is recovered. This result is notably lower than the energy penalty for power plants. In a setting where the monetary value of heat and electric power are at a similar level, the cost-of-energy for carbon dioxide capture can be in the range of -4 to 9 €/ton of carbon dioxide. From this, it follows that the operational cost of BECCS might be lower in a CHP-district heating setting than in other applications, since the total energy output from the CHP is largely preserved or even increased. Consequently, the attractiveness of BECCS could potentially increase in the context outlined in this study. As a result, the economic burden of implementation could be reduced, thereby increasing the economic efficiency of BECCS as a climate change abatement option. Thus, the need for added business value, policy instruments or other incentives to promote investments in the CCS part of BECCS may be smaller. Therefore, CHP plants could be of interest as a starting point for BECCS to finally take off as a climate mitigation tool. District heating systems with low temperatures and a small difference between the monetary value of heat and electric power are especially well equipped for development. Furthermore, when electric output is of importance, optimisation of the

capture process should be a priority. This study solely encompassed the HPC technology. For future studies, amine technology is an obvious choice for exploration, due to its high technological readiness level (Bui et al., 2018). A CHP-CCS system in a fossil-fuel setting is another avenue that could be worth investigating, to see whether it would yield similar results. Even if a fossil fueled CHP would not generate negative emissions (Kemper, 2015), it could be part of a climate mitigation strategy. It would also be of interest to see what results a similar study on industrial CHPs would generate, as such CHPs operate under different conditions and have different requirements on energy delivery.

## Data availability

The data, which this study is based on, will be made available on reasonable request.

## Funding

This study was made possible through cooperation between the Royal Institute of Technology (KTH) and Stockholm Exergi AB, which is co-owned by the Fortum Oy group and the City of Stockholm. The study was co-financed by the Swedish Energy Agency through grant number 49101-1.

## References

Al-Ramdhan, H.A., 2001. A Rate-Based Model for the Design and Simulation of a Carbon Dioxide Absorber Using the Hot Potassium Carbonate Process. Colorado School of Mines, Golden, Colorado.

Artanto, Y., Jansen, J., Pearson, P., Do, T., Cottrell, A., Meuleman, E., Feron, P., 2012. Performance of MEA and amine-blends in the CSIRO PCC pilot plant at Loy Yang Power in Australia. Fuel (Guildford) 101, 264–275.

Bartoo, R.K., 1984. Removing acid gas by the Benfield process. In: Presented at AIChE 1984 National Meeting. March. Atlanta, Georgia.

Benson, H.E., Field, J.H., Jimeson, R.M., 1954. $CO_2$ absorption: employing hot potassium carbonate solutions. Chem. Eng. Progr. 50, 356.

Bhave, A., Taylor, R.H.S., Fennell, P., Livingston, W.R., Shah, N., Dowell, N.M., Dennis, J., Kraft, M., Pourkashanian, M., Insa, M., Jones, J., Burdett, N., Bauen, A., Beal, C., Smallbone, A., Akroyd, J., 2017. Screening and techno-economic assessment of biomass-based power generation with CCS technologies to meet 2050 $CO_2$ targets. Appl. Energy 190, 481–489.

Bohloul, M.R., Peyghambarzadeh, S.M., Lee, A., Vatani, A., 2014. Experimental and analytical study of solubility of carbon dioxide in aqueous solutions of potassium carbonate. Int. J. Greenh. Gas Control. 29, 169–175.

Bohloul, M.R., Arab Sadeghabadi, M., Peyghambarzadeh, S.M., Dehghani, M.R., 2017. $CO_2$ absorption using aqueous solution of potassium carbonate: experimental measurement and thermodynamic modeling. Fluid Phase Equilib 447, 132–141.

Borhani, T.N.G., Azarpour, A., Akbari, V., Wan Alwi, S.R., Manan, Z.A., 2015. $CO_2$ capture with potassium carbonate solutions: a state-of-the-art review. Int. J. Greenh. Gas Control. 41, 142–162.

Bryngelsson, M., Westermark, M., 2009. $CO_2$ capture pilot test at a pressurized coal fired CHP plant. Energy Procedia 1, 1403–1410.

Budinis, S., Krevor, S., Dowell, N.M., Brandon, N., Hawkes, A., 2018. An assessment of CCS costs, barriers and potential. Energy Strategy Rev 22, 61–81.

Bui, M., Fajardy, M., Dowell, N.M., 2017a. Thermodynamic evaluation of carbon negative power generation: bio-energy CCS (BECCS). Energy Procedia 114, 6010–6020.

Bui, M., Fajardy, M., Mac Dowell, N., 2017b. Bio-energy with CCS (BECCS) performance evaluation: efficiency enhancement and emissions reduction. Appl. Energy 195, 289–302.

Bui, M., Adjiman, C.S., Bardow, A., Anthony, E.J., Boston, A., 2018. Carbon capture and storage (CCS): the way forward. Energy Environ. Sci. 11, 1062–1176.

Bui, M., Fajardy, M., Zhang, D., Mac Dowell, N., 2020. Delivering Negative Emissions From Biomass-Derived Hydrogen. H2FC SUPERGEN, London, UK.

Cabral, R.P., Mac Dowell, N., 2017. A novel methodological approach for achieving £/MWh cost reduction of $CO_2$ capture and storage (CCS) processes. Appl. Energy 205, 529–539.

Cabral, R.P., Bui, M., Mac Dowell, N., 2019. A synergistic approach for the simultaneous decarbonisation of power and industry via bioenergy with carbon capture and storage (BECCS). Int. J. Greenh. Gas Control. 87, 221–237.

Clarke, L.K.J., Akimoto, K., Babiker, M., Blanford, G., Fisher-Vanden, K., Hourcade, J.-C., Krey, V., Kriegler, E., Löschel, A., McCollum, D., Paltsev, S., Rose, S., Shukla, P.R., Tavoni, M., van der Zwaan, B.C.C., van Vuuren, D.P., 2014. Assessing transformation pathways. In: Edenhofer, O., Pichs-Madruga, R., Sokona, Y., Farahani, E., Kadner, S., Seyboth, K., Adler, A., Baum, I., Brunner, S., Eickemeier, P., Kriemann, B., Savolainen, J., Schlömer, S., von Stechow, C., Zwickel, T., Minx, J.C. (Eds.). Climate Change 2014: Mitigation of Climate Change. Contribution of Working Group III to the Fifth Assessment Report of the Intergovernmental Panel on Climate Change. Cambridge University Press, Cambridge, United Kingdom and New York, NY, USA.

Emenike, O., Michailos, S., Finney, K.N., Hughes, K.J., Ingham, D., Pourkashanian, M., 2020. Initial techno-economic screening of BECCS technologies in power generation for a range of biomass feedstock Sustain. Energy Technol. Assess. 40, 100743.

Equinor, 2020. Pressure and Temperature Requirements for Transport and Geological Storage of Carbon Dioxide in the Northern Lights Project Personal communication with Aasen, E.Y., February, 2020.

Fosbøl, P., von Solms, N., Gladis, A., Thomsen, K., Kontogeorgis, G.M., 2017. Methods and Modelling for Post-Combustion $CO_2$ Capture in Process Systems and Materials for $CO_2$ Capture. Wiley, New York.

Fridahl, M., 2017. Socio-political prioritization of bioenergy with carbon capture and storage. Energy Policy 104, 89–99.

Gadd, H., Werner, S., 2014. Achieving low return temperatures from district heating substations. Appl. Energy 136, 59–67.

Global CCS Institute, 2019. Bioenergy and Carbon Capture and Storage. (accessed March, 15, 2020). https://www.globalccsinstitute.com/resources/publications-reports-research/bioenergy-and-carbon-capture-and-storage/.

Gough, C., Thornley, P., Mander, S., Vaughan, N., Lea-Langton, A., 2018. Biomass Energy with Carbon Capture and Storage (BECCS): Unlocking Negative Emissions. John Wiley & Sons, Incorporated, Newark, New Jersey.

Gregory, F.N., Max, W.C., Felix, C., Sabine, F., Jens, H., Jérôme, H., William, F.L., Jan, C. M., Sophia, R., Pete, S., 2018. Negative emissions—part 3: innovation and upscaling. Environ. Res. Lett. 13, 063003.

Gustafsson, K., 2018. Spearheading Negative Emissions in Stockholm's Multi-Energy System in Bioenergy with Carbon Capture and Storage: From Global Potentials to Domestic Realities. ELF, Brussels.

Harkin, T., Hoadley, A., Hooper, B., 2011. Using multi-objective optimisation in the design of $CO_2$ capture systems for retrofit to coal power stations. Energy 41, 228–235.

Hoegh-Guldberg, O.D.J., Taylor, M., Bindi, M., Brown, S., Camilloni, I., Diedhiou, A., Djalante, R., Ebi, K., Engelbrecht, F., Guiot, J., Hijioka, Y., S.M, Payne, A., Seneviratne, S.I., Thomas, A., Warren, R., Zhou, G., 2018. Impacts of 1.5°C global warming on natural and human systems. In: Masson-Delmotte, V., Zhai, P., Pörtner, H.O., Roberts, D., Skea, J., Shukla, P.R., Pirani, A., Moufouma-Okia, W., Péan, C., Pidcock, R., Connors, S., Matthews, J.B.R., Chen, Y., Zhou, X., Gomis, M.I., Lonnoy, E., Maycock, T., Tignor, M., Waterfield, T. (Eds. Global Warming of 1.5°C. An IPCC Special Report on the Impacts of Global Warming of 1.5°C Above pre-Industrial Levels and Related Global Greenhouse Gas Emission Pathways, in the Context of Strengthening the Global Response to the Threat of Climate Change, Sustainable Development, and Efforts to Eradicate Poverty. In Press.

Honegger, M., Reiner, D., 2017. The political economy of negative emissions technologies: consequences for international policy design. Clim. Policy 18, 306–321.

IPCC, 2018. Summary for policymakers. In: Masson-Delmotte, V., Zhai, P., Pörtner, H.O., Roberts, D., Skea, J., Shukla, P.R., Pirani, A., Moufouma-Okia, W., Péan, C., Pidcock, R., Connors, S., Matthews, J.B.R., Chen, Y., Zhou, X., Gomis, M.I., Lonnoy, E., Maycock, T., Tignor, M., Waterfield, T. (Eds.). Global Warming of 1.5°C. An IPCC special report on the Impacts of Global Warming of 1.5°C Above pre-Industrial Levels and Related Global Greenhouse Gas Emission Pathways, in the Context of Strengthening the Global Response to the Threat of Climate Change. Sustainable Development, and Efforts to Eradicate Poverty. World Meteorological Organization, Geneva, Switzerland, 32 pp.

Isa, F., Zabiri, H., Ng, N.K.S., Shariff, A.M., 2018. $CO_2$ removal via promoted potassium carbonate: a review on modeling and simulation techniques. Int. J. Greenh. Gas Control. 76, 236–265.

iwb, 2020. (accessed March, 15, 2020). https://www.iwb.ch/Ueber-uns/Projekte/Temperaturabsenkung-Fernw-rmenetz.html.

Kather, A.L.U., Ehlers, S., 2016. Power Plant Integration Methods for Liquid Absorbent-Based Post-Combustion $CO_2$ Capture in Absorption Based Post-Combustion Capture of Carbon Dioxide. Woodhead Publishing, Duxford.

Kemper, J., 2015. Biomass and carbon dioxide capture and storage: a review. Int. J. Greenh. Gas Control. 40, 401–430.

Kohl, A.L., Nielsen, R.B., 1997. Alkaline Salt Solutions for Acid Gas Removal in Gas Purification. Gulf Pub, Houston.

Kuramochi, T., Faaij, A., Ramírez, A., Turkenburg, W., 2010. Prospects for cost-effective post-combustion $CO_2$ capture from industrial CHPs. Int. J. Greenh. Gas Control. 4, 511–524.

Levihn, F., 2017. CHP and heat pumps to balance renewable power production: lessons from the district heating network in Stockholm. Energy 137, 670–678.

Levihn, F., Linde, L., Gustafsson, K., Dahlen, E., 2019. Introducing BECCS through HPC to the research agenda: the case of combined heat and power in Stockholm. Energy Rep 5, 1381–1389.

Lund, H., Østergaard, P.A., Chang, M., Werner, S., Svendsen, S., Sorknæs, P., Thorsen, J. E., Hvelplund, F., Mortensen, B.O.G., Mathiesen, B.V., Bojesen, C., Duic, N., Zhang, X., Möller, B., 2018. The status of 4th generation district heating: research and results. Energy 164, 147–159.

Milidovich, S.P.E., Zbacknick, E., 2013. Increasing Efficiency of Hot Potassium Carbonate $CO_2$ Removal Systems. Honeywell UOP.

Moullec, Y.L., Neveux, T., 2016. Process Modifications for $CO_2$ Capture in Absorption-Based Post-Combustion Capture of Carbon Dioxide. Woodhead Publishing, Duxford, pp. 305–340.

Mumford, K.A., Smith, K.H., Anderson, C.J., Shen, S., Tao, W., Suryaputradinata, Y.A., Qader, A., Hooper, B., Innocenzi, R.A., Kentish, S.E., Stevens, G.W., 2012. Post-combustion capture of $CO_2$: results from the solvent absorption capture plant at

Hazelwood power station using potassium carbonate solvent. Energy Fuels 26, 138–146.
Mumford, K.A., Wu, Y., Smith, K.H., Stevens, G.W., 2015. Review of solvent based carbon-dioxide capture technologies. Front. Chem. Sci. Eng. 9, 125–141.
Neveux, T., Le Moullec, Y., Favre, É., 2017. Post-Combustion $CO_2$ Capture by Chemical Gas–Liquid Absorption: Solvent Selection, Process Modelling, Energy Integration and Design Methods in Process Systems and Materials for $CO_2$ Capture. Wiley, New York.
Oexmann, J., Kather, A., 2010. Minimising the regeneration heat duty of post-combustion $CO_2$ capture by wet chemical absorption: the misguided focus on low heat of absorption solvents. Int. J. Greenh. Gas Control. 4, 36–43.
Ooi, S.M.P., 2008. Development and Demonstration of a New Non-Equilibrium Rate-based Process Model for the Hot Potassium Carbonate Process. University of Adelaide.
Page, S.C., Williamson, A.G., Mason, I.G., 2009. Carbon capture and storage: fundamental thermodynamics and current technology. Energy Policy 37, 3314–3324.
Pour, N., Webley, P.A., Cook, P.J., 2018. Potential for using municipal solid waste as a resource for bioenergy with carbon capture and storage (BECCS). Int. J. Greenh. Gas Control. 68, 1–15.
Puxty, G., Maeder, M., 2016. The Fundamentals of Post Combustion Capture in Absorption-Based Post-Combustion Capture of Carbon Dioxide. Woodhead Publishing, p. 4. Duxford p.
Sanchez, D.L., Callaway, D.S., 2016. Optimal scale of carbon-negative energy facilities. Appl. Energy 170, 437–444.
Skorek-Osikowska, A., Bartela, Ł., Kotowicz, J., 2017. Thermodynamic and ecological assessment of selected coal-fired power plants integrated with carbon dioxide capture. Appl. Energy 200, 73–88.
Smith, K.H., Anderson, C.J., Tao, W., Endo, K., Mumford, K.A., Kentish, S.E., Qader, A., Hooper, B., Stevens, G.W., 2012. Pre-combustion capture of $CO_2$—results from solvent absorption pilot plant trials using 30wt% potassium carbonate and boric acid promoted potassium carbonate solvent. Int. J. Greenh. Gas Control. 10, 64–73.
Smith, K., Xiao, G., Mumford, K., Gouw, J., Indrawan, I., Thanumurthy, N., Quyn, D., Cuthbertson, R., Rayer, A., Nicholas, N., Lee, A., Silva, da, G., Kentish, S., Harkin, T., Qader, A., Anderson, C., Hooper, B., Stevens, G., 2014. Demonstration of a concentrated potassium carbonate process for $CO_2$ Capture. Energy Fuels 28, 299–306.
Smith, K.H., Nicholas, N.J., Stevens, G.W., 2016. Inorganic Salt Solutions for Post-Combustion Capture in Absorption-Based Post-Combustion Capture of Carbon Dioxide. Woodhead Publishing, Duxford.
Speight, J.G., 2019. Gas Cleaning Processes in Natural Gas. Gulf Professional Publishing, Boston.
Stockholm Exergi, 2016. Performance Test on CHP 8 at Värtaverket in Stockholm.
Tosh, J.S., 1959. Equilibrium Study of the System Potassium Carbonate, Potassium Bicarbonate, Carbon Dioxide, and Water. United States Bureau of Mines.
Tumilar, A., Sharma, M., Milani, D., Abbas, A., 2016. Modeling and simulation environments for sustainable low-carbon energy production – a review. Chem. Prod. Process. Model. 11, 97–124.
Turton, R., Whiting, W.B., Shaeiwitz, J.A., Bhattacharyya, D., 2018. Analysis, Synthesis, and Design of Chemical Processes. Prentice Hall, 1 ed.
Wu, Y., Wu, F., Hu, G., Mirza, N.R., Stevens, G.W., Mumford, K.A., 2018. Modelling of a post-combustion carbon dioxide capture absorber using potassium carbonate solvent in Aspen Custom Modeller. Chin. J. Chem. Eng. 26, 2327–2336.

## *Further reading*

Edenhofer, O., Pichs-Madruga, R., Sokona, Y., Farahani, E., Kadner, S., Seyboth, K., Adler, A., Baum, I., Brunner, S., Eickemeier, P., Kriemann, B., Savolainen, J., Schlömer, S., von Stechow, C., Zwickel, T., Minx, J.C., 2014. Climate Change 2014: Mitigation of Climate Change. Contribution of Working Group III to the Fifth Assessment Report of the Intergovernmental Panel on Climate Change. IPCC. Cambridge, United Kingdom and.